

Longitudinal study of sodium MRI of articular cartilage in patients with knee osteoarthritis: initial experience with 16-month follow-up

Guillaume Madelin¹ · Ding Xia¹ · Ryan Brown¹ · James Babb¹ · Gregory Chang¹ · Svetlana Krasnokutsky² · Ravinder R. Regatte¹

Received: 10 February 2017 / Revised: 15 June 2017 / Accepted: 20 June 2017 / Published online: 7 July 2017
© European Society of Radiology 2017

Abstract

Objectives To evaluate the potential of sodium MRI to detect changes over time of apparent sodium concentration (ASC) in articular cartilage in patients with knee osteoarthritis (OA).

Methods The cartilage of 12 patients with knee OA were scanned twice over a period of approximately 16 months with two sodium MRI sequences at 7 T: without fluid suppression (radial 3D) and with fluid suppression by adiabatic inversion recovery (IR). Changes between baseline and follow-up of mean and standard deviation of ASC (in mM), and their rate of change (in mM/day), were measured in the patellar, femorotibial medial and lateral cartilage regions for each subject. A matched-pair Wilcoxon signed rank test was used to assess significance of the changes.

Results Changes in mean and in standard deviation of ASC, and in their respective rate of change over time, were only statistically different when data was acquired with the fluid-suppressed sequence. A significant decrease ($p = 0.001$) of approximately 70 mM in mean ASC was measured between the two IR scans.

Conclusion Quantitative sodium MRI with fluid suppression by adiabatic IR at 7 T has the potential to detect a decrease of ASC over time in articular cartilage of patients with knee osteoarthritis.

Key Points

- Sodium MRI can detect apparent sodium concentration (ASC) in cartilage
- Longitudinal study: sodium MRI can detect changes in ASC over time
- Potential for follow-up studies of cartilage degradation in knee osteoarthritis

Keywords Osteoarthritis · Sodium · Magnetic resonance imaging · Cartilage · Glycosaminoglycans

Abbreviations

| | |
|------------------|---|
| ¹ H | Proton |
| ²³ Na | Sodium |
| ASC | Apparent sodium concentration |
| GAG | Glycosaminoglycan |
| IR | Inversion recovery |
| IRW | IR WURST |
| KL | Kellgren–Lawrence |
| LAT | Femorotibial lateral cartilage |
| MED | Femorotibial medial cartilage |
| MRI | Magnetic resonance imaging |
| OA | Osteoarthritis |
| PAT | Patellar cartilage |
| R3D | Radial 3D |
| UTE | Ultrashort echo time |
| WURST | Wideband uniform rate and smooth truncation |

Electronic supplementary material The online version of this article (doi:10.1007/s00330-017-4956-z) contains supplementary material, which is available to authorized users.

✉ Guillaume Madelin
guillaume.madelin@nyumc.org

¹ Department of Radiology, Center for Biomedical Imaging, New York University School of Medicine, 660 First Avenue, 4th Floor, New York, NY 10016, USA

² Department of Medicine, Rheumatology Division, New York University School of Medicine, 305 Second Avenue, New York, NY 10003, USA

Introduction

Osteoarthritis (OA) is a disease of the entire joint that can result from the breakdown of articular cartilage and underlying bone, but also from broken ligaments or meniscus [1–3]. It is the most common form of arthritis and a leading cause of chronic disability in the elderly population [4]. OA is generally considered to be a degenerative disease characterised mainly by an overall loss of glycosaminoglycan (GAG) in cartilage, along with disruption of the collagen fibres and disorganization of the collagen matrix, and small increases in water content [5]. Generally, these early OA changes in GAG, collagen and water content precede the mechanical damage of cartilage and bone.

Many MRI methods [6] are being developed to provide quantitative information about the physiological changes in cartilage due to OA, such as T2 mapping [7], T1 ρ mapping [8], GAG chemical exchange saturation transfer (gagCEST) [9], delayed gadolinium-enhanced MRI of cartilage (dGEMRIC) [10], diffusion tensor imaging (DTI) [11] and sodium MRI [12]. Sodium MRI [13] has been shown to strongly correlate with the GAG concentration in the cartilage [5, 14–16]. It is therefore a promising candidate imaging biomarker for monitoring loss of GAG and cartilage degradation over time in patients with OA, and also for monitoring the effects of disease-modifying OA drugs [17].

In a previous study [18], we demonstrated that quantitative sodium MRI with fluid suppression by inversion recovery with an adiabatic pulse at 7 T in cartilage could significantly differentiate asymptomatic subjects (controls) from patients with knee OA, as it is less sensitive to partial volume effects from surrounding synovial fluid than the acquisition without fluid suppression. In the present study, which is a follow-up to the previous one [18] and is based on the same patient cohort (12 of the knee OA patients agreed to come back), we measured and compared the variations of apparent sodium concentration (ASC) in the articular cartilage with sodium MRI with and without fluid suppression by adiabatic inversion, at baseline and 16-month follow-up in patients with knee OA. The aim of this pilot study is to evaluate the potential of sodium MRI to detect changes over time of ASC in articular cartilage in patients with knee OA. The long-term goal of this work would be to assess GAG depletion in knee OA patients with longitudinal measurements of cartilage ASC using sodium MRI.

Materials and methods

Patients with OA

This study was approved by the institutional review board (IRB) and performed in compliance with the Health

Insurance Portability and Accountability Act (HIPAA). All subjects provided written informed consent. We scanned the knee cartilage of 12 patients with OA, selected from the NYU Hospital of Joint Diseases knee OA cohort [19]. Subject characteristics are provided in Table 1. These patients fulfilled the clinical OA symptoms defined by the American College of Rheumatology [20] (ACR) as well as radiographic evidence of tibial–femoral knee OA with Kellgren–Lawrence (KL) grade of 1–4 on the standardized weight-bearing fixed-flexion posterior–anterior knee radiographs at baseline [21]. The exclusion criteria were any inflammatory arthritis, prior traumatic knee injury or surgery on either knee, or history of bilateral knee replacements.

Hardware

All sodium images were acquired on a whole-body 7 T scanner (Siemens Healthcare, Erlangen, Germany) with a homemade double-tuned proton–sodium knee coil [22] (4-channel transmit–receive for proton, birdcage transmit and 8-channel receive for sodium).

Sodium MRI acquisition

MRI sequences

Sodium images without fluid suppression were acquired using an ultrashort echo time (UTE) radial 3D sequence (R3D) [23]. Fluid suppression was obtained by inversion recovery (IR) using an adiabatic pulse and appropriate inversion time prior to the R3D sequence [24]. The adiabatic pulse was the WURST (wideband uniform rate and smooth truncation) pulse [25] with a sweep range of 2 kHz and the sequence is referred to as IR WURST (IRW). The sequences were written in SequenceTree 4.2.2 [26] and compiled with the Siemens program IDEA VB15A/VB17A. All sequence parameters, imaging gradients and RF pulses were exactly the same for the two scans. Images were reconstructed offline in Matlab (Mathworks, Natick, MA, USA) using a non-uniform fast Fourier transform (NUFFT) algorithm [27]. Details of the sequences and reconstruction parameters are presented in Table 2.

Acquisition protocol

All subjects were scanned at baseline and follow-up with both R3D and IRW sequences. A summary flowchart of the protocol for data acquisition and analysis is presented in Supplemental Fig. S1. Data was acquired in the period November 2011–June 2012 for baseline and in the period February 2013–October 2013 for follow-up.

Table 1 Knee OA patients characteristics at baseline

| Subjects | Characteristics | Kellgren–Lawrence (KL) Grade | | | | |
|----------|-------------------|------------------------------|-------------|------------|------------|---|
| | | All | 1 | 2 | 3 | 4 |
| All | Number | 12 | 7 | 3 | 2 | 0 |
| | Mean age (years) | 65.8 ± 11.4 | 69.7 ± 12.4 | 57.7 ± 7.2 | 71.5 ± 6.4 | 0 |
| | Age range (years) | 47–81 | 47–81 | 53–66 | 67–76 | 0 |
| | Mean weight (kg) | 75.1 ± 10.9 | 73.7 ± 13.1 | 79.3 ± 9.1 | 73.5 ± 6.4 | 0 |
| | Weight range (kg) | 58–93 | 58–93 | 69–86 | 69–78 | 0 |
| Men | Number | 4 | 2 | 1 | 1 | 0 |
| | Mean age (years) | 69.3 ± 11.1 | 74.0 ± 4.2 | 53.0 ± 0.0 | 76.0 ± 0.0 | 0 |
| | Age range (years) | 53–76 | 71–77 | 53 | 76 | 0 |
| | Mean weight (kg) | 83.0 ± 8.1 | 84.0 ± 12.7 | 86.0 ± 0.0 | 78.0 ± 0.0 | 0 |
| | Weight range (kg) | 75–93 | 75–93 | 86 | 78 | 0 |
| Women | Number | 8 | 5 | 2 | 1 | 0 |
| | Mean age (years) | 66.0 ± 10.3 | 68.2 ± 13.3 | 60.0 ± 8.5 | 67.0 ± 0.0 | 0 |
| | Age range (years) | 47–81 | 47–81 | 53–66 | 67 | 0 |
| | Mean weight (kg) | 71.1 ± 10.3 | 69.6 ± 12.0 | 76.0 ± 9.9 | 69.0 ± 0.0 | 0 |
| | Weight range (kg) | 58–85 | 58–85 | 69–83 | 69 | 0 |

Image post-processing

Apparent sodium concentration maps

All sodium images were acquired in the presence of calibration phantoms made of 4% Agar gel with known sodium concentrations (100, 150, 200, 250 and 300 mM). After T1 and T2* correction of the phantom signal intensities (T1 = 23 ms, T2*_{short} = 2 ms, T2*_{long} = 12 ms), ASC maps were calculated using linear regression [18, 24], which was considered valid only when the coefficient of determination R² was at least 0.99, to improve robustness of the method against

noise and phantom signal variations [28]. The ASC maps were then corrected for average T1 and T2* of cartilage in vivo (T1 = 20 ms, T2*_{short} = 1 ms, T2*_{long} = 13 ms) to increase accuracy of the quantification of sodium concentration in cartilage [29]. Since, on average, 25% of the volume in cartilage is made up of solids without any sodium, the final sodium maps were divided by a factor 0.75 [18, 30, 31].

Image co-registration

For each subject, all four 3D datasets (R3D and IRW from baseline and follow-up) were co-registered using 3D Voxel

Table 2 Sodium acquisition sequence and reconstruction parameters

| Parameters | Unit | Radial 3D (R3D) | IR WURST (IRW) |
|-------------------------------------|--------|-----------------|----------------|
| Number of radial projections | – | 10,000 | 10,000 |
| Repetition time (TR) | ms | 100 | 140 |
| Echo time (TE) | ms | 0.4 | 0.4 |
| Flip angle (FA) | degree | 90 | 90 |
| Isotropic field of view (FOV) | mm | 200 | 200 |
| Dwell time | μs | 80 | 80 |
| Adiabatic inversion pulse amplitude | Hz | – | 240 |
| Adiabatic inversion pulse length | ms | – | 10 |
| Inversion time (TI) | ms | – | 24 |
| Nominal resolution* | mm | 2 | 2 |
| Real resolution** | mm | 3.3 | 3.3 |
| Acquisition time (TA) | min:s | 16:44 | 23:25 |

* The nominal (reconstructed) resolution is the size of the isotropic voxels chosen in the regridding algorithm for reconstructing the images from the 3D radial k-space trajectory

** The real resolution is the resolution calculated from the usual resolution formula: resolution = 1/(2 × k_{max}), with k_{max} the maximal value of the k-space used for reconstructing the images

Registration in Analyze 10.0 (AnalyzeDirect Inc., Overland Park, KS).

ASC measurements

Three regions-of-interest (ROI) of 40 pixels were drawn on the patellar (PAT), femorotibial lateral (LAT) and femorotibial medial (MED) cartilage, on eight consecutive slices of the ASC maps using the following protocol for each subject: (1) For each consecutive slice, draw a large ROI surrounding the cartilage area where we want to make the measurement; (2) On the first R3D data (baseline), select 40 pixels with highest ASC values within the large ROI; (3) Generate a mask from this 40-pixel area; (4) Transpose this mask to all other three co-registered datasets (baseline IRW, follow-up R3D and follow-up IRW); (5) Measure the pixels values corresponding to the mask in each dataset; (6) Calculate the mean and standard deviation (std) of ASC over all 320 pixels (eight ROIs of 40 pixels). Examples of ROIs and masks to measure ASC values in PAT (transverse slice), MED and LAT (coronal slice) are shown in Fig. 1. This procedure ensures that all the ASC values are measured at exactly the same locations in all 3D sodium datasets for each subject.

RF coil correction

A signal-to-noise ratio (SNR) map of the coil was calculated on a uniform cylindrical water phantom doped with 45 mM of NaCl that filled the coil volume [22], from an R3D acquisition with 15,000 projections and other parameters from Table 2. The SNR distribution was highest in the periphery and reduced toward the centre, which is typical of phased array coils (see Brown et al. [22] for the map), and therefore was used to correct the images from all subjects prior to ASC quantification [18].

Statistical analysis

For each subject the change in each measure (mean or std of ASC, in mM) from each region as determined by each sequence was computed as the value at baseline minus the value at follow-up. As a result, positive change corresponds to a decline in value over time. The regional rate of change in each measure was computed for each subject as the change divided by the time between scans for that subject. Rates of change are expressed in units of mM/day. For each measure within each region the matched-pair Wilcoxon signed rank test was used to assess whether the measure changed over time and to compare sequences in terms of the change over time and the rate of change. Exact Mann–Whitney tests were used to compare male and female patients in terms of the change and rate of change in each regional measure. Spearman rank correlations were used to assess the relationship of the change and rate of

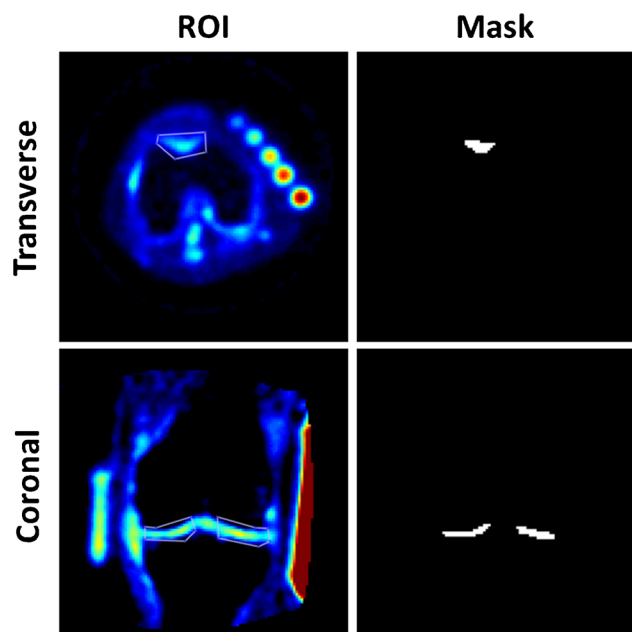


Fig. 1 Examples of large regions-of-interest (ROIs) and masks generated from 40 pixels with the highest values within the large ROIs, on a transverse slice showing patellar cartilage (PAT), and on a coronal slice showing femorotibial lateral (LAT) and medial (MED) cartilage. These large ROIs and masks are generated on the first dataset acquired on each subject (R3D at baseline). These masks are then transposed to the three other co-registered datasets (baseline R3D, follow-up R3D, follow-up IRW) where all 40 corresponding pixel values are measured. This procedure ensures that all the ASC values are measured at exactly the same locations in all 3D sodium datasets for each subject

change in each regional measure with age, weight and KL score. Statistical significance is defined as a p value less than 0.05. All statistical tests were conducted at the two-sided 5% significance level using SAS 9.3 (SAS Institute, Cary, NC).

Results

Sodium concentration maps

Figure 2 shows representative transverse and coronal ASC maps through the knee cartilage from the same OA patient (KL = 1) at baseline (scan 1) and follow-up (scan 2, mean delay = 478 days, i.e. approximately 16 months later), calculated from radial 3D (R3D, no fluid suppression) and IR WURST (IRW, fluid suppression) acquisitions. The ASC measured with R3D look very similar in both scans, while a greater difference in ASC can be visually detected with IRW in all three cartilage regions.

Figure 3 shows the distributions of the ASC values measured in all voxels of all the ROIs of all subjects, from R3D and IRW acquisitions, for individual cartilage compartments (PAT, MED, LAT). We can visually detect a slight overall shift to the left (lower ASC) between scan 1 and 2 for the R3D

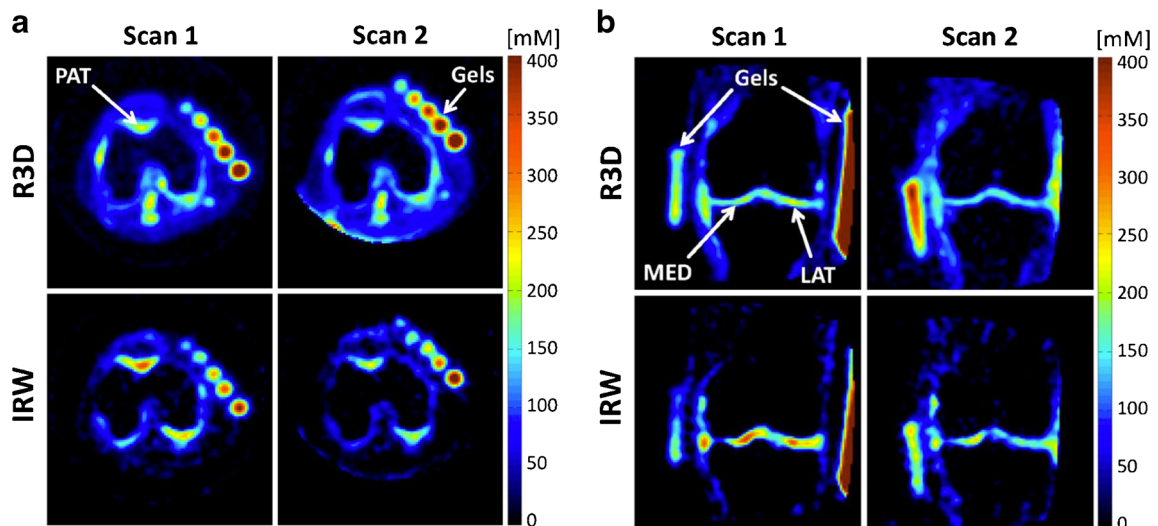


Fig. 2 Sodium maps from one OA patient, reconstructed from data acquired with fluid suppression (sequence IRW) and without fluid suppression (sequence R3D), at baseline (scan 1) and 16-month follow-up (scan 2). **a** Transverse slices showing patellar cartilage (PAT). **b**

Coronal slices showing femorotibial lateral (LAT) and medial (MED) cartilage. The apparent sodium concentrations (ASC) measured with R3D look very similar in both scans, while a higher difference of ASC can be detected visually with IRW in PAT, MED and LAT

measurements, while this shift is noticeably larger for the IRW measurements.

Figure 4 shows box plots of mean and std of ASC measured in PAT, MED and LAT compartments and calculated from R3D and IRW acquisitions, for all OA patients, at baseline (scan 1) and follow-up (scan 2). All ASC measures (mean and std) in all compartments show a statistically significant

decrease between baseline and follow-up when calculated from IRW acquisitions. When data is acquired using R3D, only the mean ASC in LAT compartment shows a significant decrease. See Table 3 for statistics.

Figure 5 shows scatter plots of mean and std of ASC measured in PAT, MED and LAT compartments, and calculated from R3D and IRW acquisitions, for all OA patients: baseline

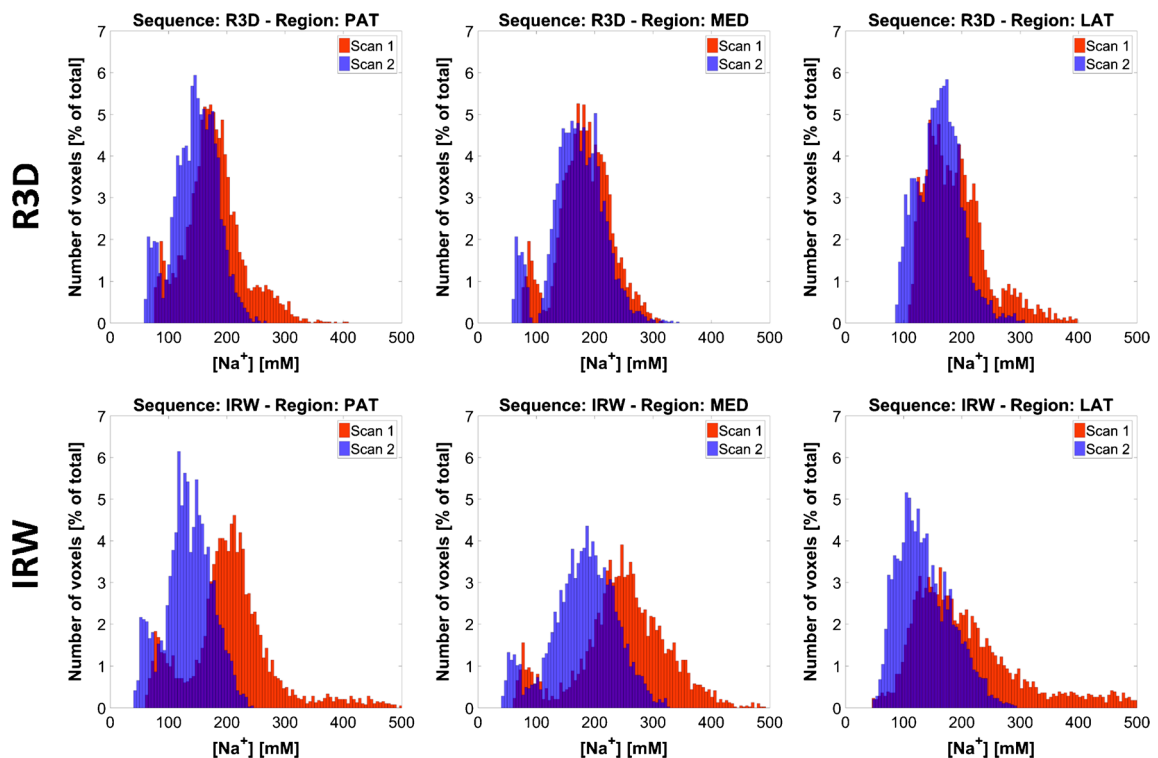


Fig. 3 Distribution (histograms) of the apparent sodium concentrations (ASC) measured in all voxels of all the ROIs of all subjects, from R3D acquisition (no fluid suppression) and from IRW acquisition (fluid suppression), for individual cartilage compartments (PAT, MED, LAT)

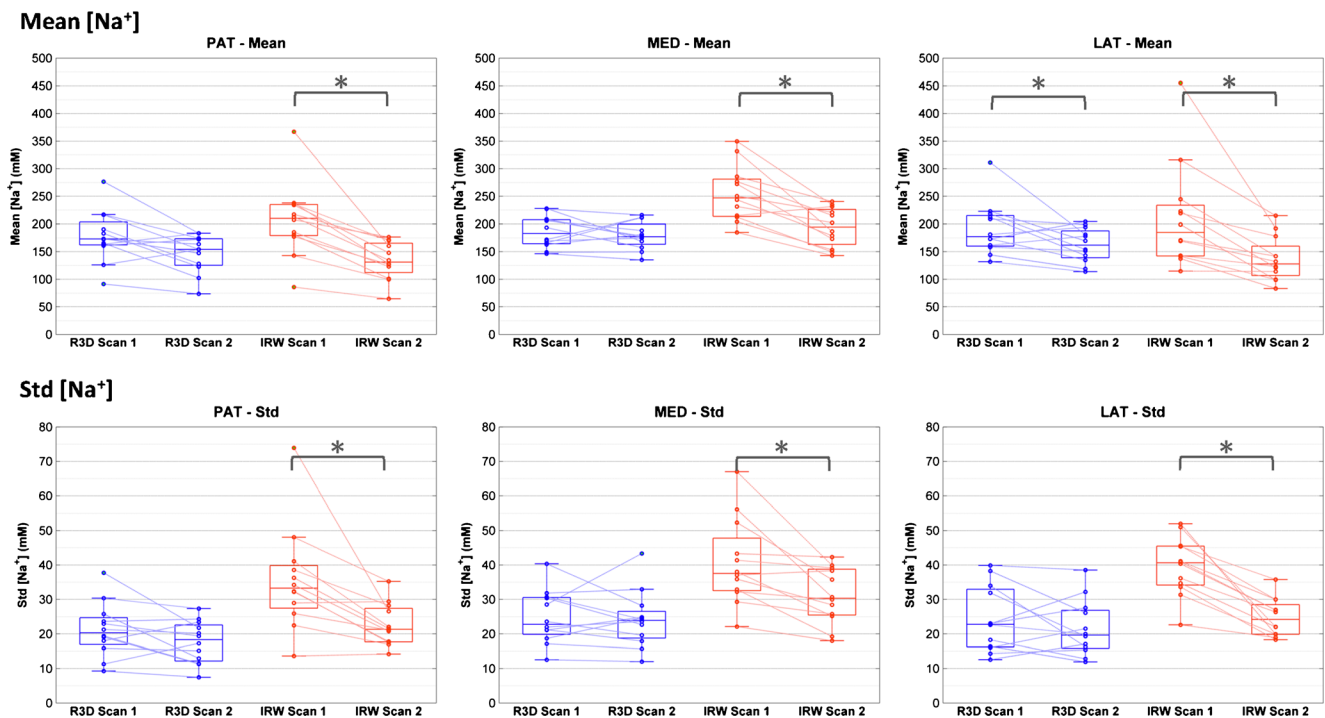


Fig. 4 Box plots of mean and standard deviation (std) of apparent sodium concentration (ASC) measured in PAT, MED and LAT cartilage compartments and calculated from R3D (blue) and IRW (red) acquisitions, for all 12 OA patients, at baseline (scan 1) and 16-month follow-up (scan 2). *Statistical significance ($P < 0.05$)

Table 3 Statistics of the intrasubject change in each measure of apparent sodium concentration (ASC) in mM, and the rate of change in each measure of ASC in mM/day, within each cartilage region as determined using each sequence

| Measure | Region | IR WURST | | | | | Radial 3D | | | | |
|---|--------|----------|-------|--------|-------|--------------|-----------|-------|--------|-------|--------------|
| | | Mean | Std | Median | IQR | <i>p</i> | Mean | Std | Median | IQR | <i>p</i> |
| Change in measure of ASC (mM)* | | | | | | | | | | | |
| Mean | LAT | 72.73 | 71.02 | 48.15 | 70.63 | 0.001 | 29.48 | 44.90 | 21.70 | 69.62 | 0.034 |
| Mean | MED | 67.53 | 35.32 | 61.95 | 48.35 | 0.001 | 7.18 | 30.92 | 11.10 | 46.33 | 0.519 |
| Mean | PAT | 73.29 | 48.81 | 64.00 | 40.85 | 0.001 | 31.42 | 38.55 | 34.25 | 68.48 | 0.052 |
| Std | LAT | 14.82 | 8.02 | 13.05 | 5.33 | 0.002 | 2.63 | 8.29 | 2.00 | 15.10 | 0.077 |
| Std | MED | 9.58 | 9.54 | 5.80 | 13.60 | 0.002 | 0.83 | 7.11 | 1.00 | 9.05 | 0.583 |
| Std | PAT | 13.08 | 12.64 | 13.10 | 9.85 | 0.001 | 3.57 | 6.66 | 2.45 | 8.20 | 0.391 |
| Rate of change in measure of ASC (mM/day)** | | | | | | | | | | | |
| Mean | LAT | 0.149 | 0.084 | 0.138 | 0.087 | 0.001 | 0.064 | 0.076 | 0.072 | 0.146 | 0.027 |
| Mean | MED | 0.139 | 0.065 | 0.125 | 0.098 | 0.001 | 0.014 | 0.062 | 0.025 | 0.098 | 0.519 |
| Mean | PAT | 0.145 | 0.125 | 0.105 | 0.151 | 0.001 | 0.058 | 0.086 | 0.047 | 0.152 | 0.052 |
| Std | LAT | 0.026 | 0.022 | 0.028 | 0.021 | 0.002 | 0.007 | 0.014 | 0.005 | 0.018 | 0.077 |
| Std | MED | 0.020 | 0.020 | 0.013 | 0.025 | 0.002 | 0.002 | 0.015 | 0.002 | 0.017 | 0.622 |
| Std | PAT | 0.030 | 0.014 | 0.028 | 0.012 | 0.001 | 0.005 | 0.017 | 0.004 | 0.032 | 0.380 |

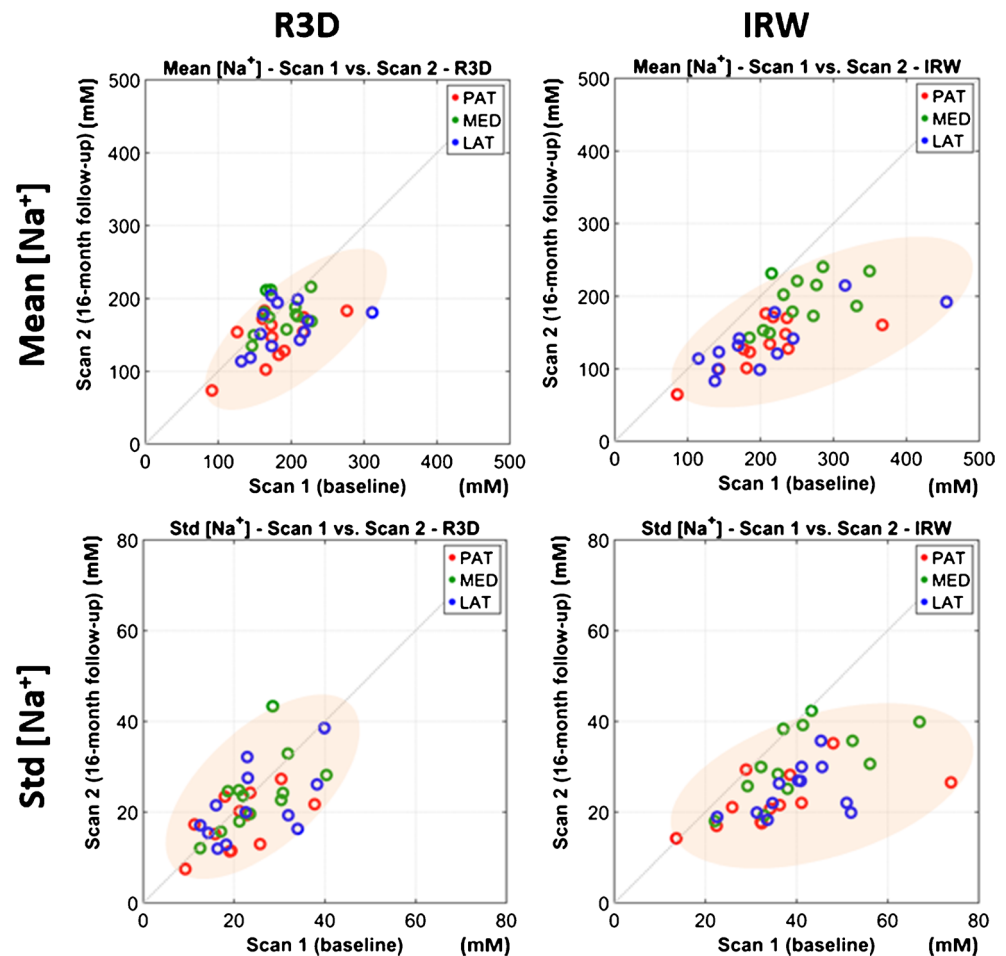
p values in bold font represent statistical significance ($p < 0.05$)

PAT patellar cartilage, MED femorotibial medial cartilage, LAT femorotibial lateral cartilage, Std standard deviation, IQR interquartile range

* Each *p* value is calculated from the Wilcoxon test to assess whether the measure changed over time

** Each *p* value is calculated from the Wilcoxon test to assess whether the rate of change in the measure differed from zero

Fig. 5 Scatter plots of mean and standard deviation (std) of apparent sodium concentration (ASC) measured in PAT, MED and LAT cartilage compartments, and calculated from R3D (blue) and IRW (red) acquisitions, for all 12 OA patients: baseline (scan 1) vs. 16-month follow-up (scan 2)



(scan 1) vs. follow-up (scan 2). We can notice that for R3D, all data points are close to the diagonal (no change in measurement), while for IRW most of the data points are below the diagonal (decrease in measurement).

Statistical analysis

The time between scans of each patient had a mean \pm std of 477.67 ± 33.3 days (min–max range = 417–582 days) with a coefficient of variation (CV) of 8.0%. This small CV implies that results based on change and rate of change of ASC will be highly consistent in terms of correlations and p values.

Table 3 presents the mean, std, median and interquartile range (IQR) of the within-subject change in each measure of ASC in mM, and the rate of change in each measure of ASC in mM/day, within each cartilage region as determined using each sequence. Each p value is calculated to assess whether the measure changed over time or whether the rate of change in the measure differed from zero. All changes of mean and std of ASC, and rates of change of mean and std of ASC, over the follow-up delay, were statistically significant for all cartilage compartments when measured using IRW. R3D data shows a

significant decrease only for the mean ASC and for the rate of change in mean ASC in the patellar cartilage. For IRW, decrease in mean ASC was in the range 67.5–73.3 mM, and decrease in std of ASC was in the range 9.6–14.8 mM, in whole cartilage. For R3D, the decrease in mean ASC was much smaller (less than half of IRW), in the range 7.2–31.4 mM, and the decrease in std of ASC was also very small compared to IRW, in the range 0.8–3.6 mM. Rates of changes for IRW were in the range 0.139–0.149 mM/day for mean ASC, and 0.020–0.030 mM/day for std of ASC. Rates of changes in mean and std of ASC from R3D were also much smaller than from IRW, in the range 0.014–0.064 mM/day and 0.002–0.007 mM/day, respectively.

Complementary results from the statistical analysis are shown in Tables S1–S4 of the Supplemental Material. Table S1 presents the mean, std, median and IQR of the within-subject difference between sequences (IRW minus R3D) in terms of the change in each measure of ASC in mM, and in terms of the rate of change in each measure of ASC in mM/day, within each cartilage region. In all cases the sequences differed significantly for change of mean and std of ASC, and for rate of change of mean and std of ASC over

time, for each subject. Table S2 presents the mean, std, median and IQR of the within-subject change in each measure of ASC within each cartilage region as determined using each sequence for each gender. No significant difference was detected between measurements in male and female patients, except for the measure of std of ASC from R3D in PAT. Table S3 presents the mean, std, median and IQR of the within-subject rate of change in each measure of ASC within each cartilage region as determined using each sequence for each gender. No significant difference was detected between measurements in male and female patients, except for the measure of std of ASC from R3D in PAT. Table S4 presents the Spearman correlation (R) and p value for the association of the change and rate of change in each regional measure of ASC with age, weight and KL grade. No correlation was found significant between age and any change or rate of change in the measures of mean and std of ASC. A significant correlation was found between KL grade and change in mean ASC in LAT ($R = 0.69$, $p = 0.013$), and between KL grade and change in std of ASC in MED ($R = 0.79$, $p = 0.002$), for IRW acquisition only. Similar correlations between KL grades and the rates of change in measures of ASC in the same cartilage regions were noticed for IRW data. A significant correlation was found between weight and change in mean ASC ($R = 0.65$, $p = 0.023$), in PAT for R3D acquisition. Significant correlation were noticed between weight and the rate of change in mean ASC in PAT from R3D ($R = 0.64$, $p = 0.025$), the rate of change in std of ASC in PAT from R3D ($R = 0.61$, $p = 0.037$) and the rate of change in std of ASC in MED from IRW ($R = 0.58$, $p = 0.046$).

Discussion

From the results presented in Table 3, we can assert that measurements of the changes in mean ASC and in std of ASC, and in their respective rate of change over time, were only statistically different between baseline and follow-up when data was acquired with the fluid-suppressed sequence IRW. Moreover, for each subject, the difference in all results from IRW and R3D was significantly different, with the changes measured from IRW data much larger (by at least a factor 2) than the changes measured from R3D data. This is mainly due to a reduction of partial volume effect of the surrounding synovial fluid ($[Na^+] \sim 140$ mM) by inversion recovery.

Acquiring sodium data with MRI is challenging because the sodium MR signal in cartilage is about 3500 times lower than the proton signal, and exhibits very fast relaxation that necessitates specific ultrashort echo time (UTE) acquisition sequences such as radial 3D [13]. As a result of these challenges, sodium MRI is generally acquired with low resolution (3.3 mm isotropic in our case, which is similar to the thickness of human knee cartilage [32]) and long acquisition times

(16 min for R3D and 23 min for IRW) at 7 T. We showed that IRW reduces partial volume effects of surrounding fluids associated with the coarse resolution. Going forward, this method could be implemented with more efficient UTE 3D sequences such as FLORET [33] or TPI [34] which can increase signal-to-noise efficiency by 40–50%, and exploit data undersampling and compressed sensing (CS) reconstruction [35, 36]. The combination of ultra-high field (7 T) with fast 3D acquisition with fluid suppression and optimized multi-channel CS reconstruction could allow one to acquire ASC maps with higher resolution (about 2 mm) within 10 min. On the other hand, we notice that the better performance of IRW over R3D is valid only for voxels containing cartilage and synovial fluid. For thin structures such as femoral cartilage, it might be more advantageous to trade the higher signal intensity of R3D for even higher spatial resolution (1 mm) with reduced partial volume effect from synovial fluid and other surrounding tissues.

Although the sample size was small (12 subjects), we were still able to detect longitudinal reductions in cartilage apparent sodium content, which provides support for the potential use of sodium MRI to monitor disease progression in OA. Unfortunately, progression of OA could not be assessed in these patients, and KL grades at follow-up were therefore not available for comparison with baseline and for possible correlation between KL grade evolution and sodium quantification in patients. We could not confirm clinically that the level of OA progressed during follow-up. In the future, larger longitudinal studies are needed with early OA subjects, along with healthy controls, to prove that longitudinal reductions in sodium (or GAG) content can be detected with sodium IRW MRI, and have correlations with the later development of joint space narrowing on radiographs and the evolution of KL grade over time.

One limitation of this study is the lack of follow-up scans on control subjects, which could be a good indicator of the accuracy of the proposed method to detect changes in ASC in cartilage due to OA compared to normal aging. It can, however, be noticed that a CV of 8–10% can be expected for ASC quantification from IRW [37]. In this study, we measured a decrease of ASC of approximately 70 mM from baseline in the range 200–250 mM, corresponding to a variation of 28–35%. We can thus assume that this decrease is probably not due to acquisition uncertainties.

Another limitation is that, because of the small sample size, no conclusive relationship between KL grade, weight and ASC measures can be made. No significant statistical difference was found between results from male and female patients and no correlation was found between age and the measurements of mean and std of ASC.

A final limitation is that the sodium T1 and T2* relaxation times in cartilage were considered fixed in the quantification algorithm, as measured from healthy subjects in a prior study

[29]. However, these relaxation times can change during cartilage degradation [38], as a result of GAG depletion and collagen matrix deterioration, and influence ASC quantification. Measuring relaxation times in vivo can be very time consuming [29], but would bring new fundamental information about cartilage degradation. An estimation of the error propagation [24, 28, 39] of variations of T1, T2_{short} and T2_{long} of cartilage (from baseline values of 20 ms, 1 ms and 13 ms respectively [29]) of 10% each leads to a total uncertainty of 9% in mean ASC, and variations of 20% in relaxation times lead to an uncertainty of 19% in mean ASC for IRW. When no inversion is involved (R3D), the uncertainty is less than 1% in all cases. It is therefore difficult in the present study to assign which part of the loss of ASC is due to real loss of sodium content within the cartilage or due to variations of relaxation times, but it can be noticed that both are expected to be related to loss of GAG (and also collagen matrix degradation for the relaxation part) and general cartilage degradation. We will therefore keep in mind that the ASC measured with the present IRW protocol represent only an “apparent” sodium concentration that is also influenced by changes in relaxation times. Once a fast method of sodium data acquisition based on high field, efficient sequence and CS reconstruction is implemented, T1 and T2* measurement could potentially be added to the scanning protocol and help separate the effects of relaxation times on the ASC measured, along with complementary proton MRI [6].

In conclusion, this study shows that quantitative sodium MRI with fluid suppression by adiabatic inversion can detect changes in ASC over time in the articular cartilage of patients with knee OA.

Compliance with ethical standards

Guarantor The scientific guarantor of this publication is Guillaume Madelin, PhD.

Conflict of interest The authors of this manuscript declare no relationships with any companies whose products or services may be related to the subject matter of the article.

Funding This study has received funding by National Institutes of Health (grant nos. 1R01AR067156, 1R01AR060238, 1R01AR056260, 1R01AR068966, 1R03AR065763, 1R01NS097494, 1P41EB017183).

Statistics and biometry One of the authors has significant statistical expertise.

Informed consent Written informed consent was obtained from all subjects (patients) in this study.

Ethical approval Institutional review board approval was obtained.

Study subjects or cohorts overlap Some study subjects have been previously reported in Madelin G, et al. Articular cartilage: evaluation with fluid-suppressed 7.0-T sodium MR imaging in subjects with

and subjects without osteoarthritis. *Radiology*. 2013;268(2):481-91. The present study is a follow-up study of the study published in *Radiology*.

Methodology

- prospective
- longitudinal study/experimental
- performed at one institution

References

1. Sharma L (2016) Osteoarthritis year in review 2015: clinical. *Osteoarthr Cartil* 24:36–48
2. Glyn-Jones S, Palmer AJ, Agricola R, Price AJ, Vincent TL, Weinans H et al (2015) Osteoarthritis. *Lancet* 386:376–387
3. Alizai H, Roemer FW, Hayashi D, Crema MD, Felson DT, Guermazi A (2015) An update on risk factors for cartilage loss in knee osteoarthritis assessed using MRI-based semiquantitative grading methods. *Eur Radiol* 25:883–893
4. Lawrence RC, Felson DT, Helmick CG, Arnold LM, Choi H, Deyo RA et al (2008) Estimates of the prevalence of arthritis and other rheumatic conditions in the United States. Part II. *Arthritis Rheum* 58:26–35
5. Borthakur A, Mellon E, Niyogi S, Witschey W, Kneeland JB, Reddy R (2006) Sodium and T1rho MRI for molecular and diagnostic imaging of articular cartilage. *NMR Biomed* 19:781–821
6. Braun HJ, Gold GE (2012) Diagnosis of osteoarthritis: imaging. *Bone* 51:278–288
7. Smith HE, Mosher TJ, Dardzinski BJ, Collins BG, Collins CM, Yang QX et al (2001) Spatial variation in cartilage T2 of the knee. *J Magn Reson Imaging* 14:50–55
8. Regatte RR, Akella SV, Borthakur A, Kneeland JB, Reddy R (2003) In vivo proton MR three-dimensional T1rho mapping of human articular cartilage: initial experience. *Radiology* 229:269–274
9. Ling W, Regatte RR, Navon G, Jerschow A (2008) Assessment of glycosaminoglycan concentration in vivo by chemical exchange-dependent saturation transfer (gagCEST). *Proc Natl Acad Sci U S A* 105:2266–2270
10. Bashir A, Gray ML, Burstein D (1996) Gd-DTPA2- as a measure of cartilage degradation. *Magn Reson Med* 36:665–673
11. Filidoro L, Dietrich O, Weber J, Rauch E, Oerther T, Wick M et al (2005) High-resolution diffusion tensor imaging of human patellar cartilage: feasibility and preliminary findings. *Magn Reson Med* 53: 993–998
12. Reddy R, Insko EK, Noyszewski EA, Dandora R, Kneeland JB, Leigh JS (1998) Sodium MRI of human articular cartilage in vivo. *Magn Reson Med* 39:697–701
13. Madelin G, Regatte RR (2013) Biomedical applications of sodium MRI in vivo. *J Magn Reson Imaging* 38:511–529
14. Lesperance LM, Gray ML, Burstein D (1992) Determination of fixed charge density in cartilage using nuclear magnetic resonance. *J Orthop Res* 10:1–13
15. Shapiro EM, Borthakur A, Dandora R, Kriss A, Leigh JS, Reddy R (2000) Sodium visibility and quantitation in intact bovine articular cartilage using high field (23)Na MRI and MRS. *J Magn Reson* 142:24–31
16. Shapiro EM, Borthakur A, Gougoutas A, Reddy R (2002) 23Na MRI accurately measures fixed charge density in articular cartilage. *Magn Reson Med* 47:284–291
17. Qvist P, Bay-Jensen AC, Christiansen C, Dam EB, Pastoureau P, Karsdal MA (2008) The disease modifying osteoarthritis drug (DMOAD): is it in the horizon? *Pharmacol Res* 58:1–7

18. Madelin G, Babb J, Xia D, Chang G, Krasnokutsky S, Abramson SB et al (2013) Articular cartilage: evaluation with fluid-suppressed 7.0-T sodium MR imaging in subjects with and subjects without osteoarthritis. *Radiology* 268:481–491
19. Attur M, Wang HY, Kraus VB, Bukowski JF, Aziz N, Krasnokutsky S et al (2010) Radiographic severity of knee osteoarthritis is conditional on interleukin 1 receptor antagonist gene variations. *Ann Rheum Dis* 69:856–861
20. Altman R, Asch E, Bloch D, Bole G, Borenstein D, Brandt K et al (1986) Development of criteria for the classification and reporting of osteoarthritis. Classification of osteoarthritis of the knee. Diagnostic and Therapeutic Criteria Committee of the American Rheumatism Association. *Arthritis Rheum* 29:1039–1049
21. Kellgren JH, Lawrence JS (1957) Radiological assessment of osteoarthritis. *Ann Rheum Dis* 16:494–502
22. Brown R, Madelin G, Lattanzi R, Chang G, Regatte RR, Sodickson DK, Wiggins GC (2012) Design of a nested eight-channel sodium and four-channel proton coil for 7T knee imaging. *Magn Reson Med* (in press)
23. Nielles-Vallespin S, Weber MA, Bock M, Bongers A, Speier P, Combs SE et al (2007) 3D radial projection technique with ultrashort echo times for sodium MRI: clinical applications in human brain and skeletal muscle. *Magn Reson Med* 57:74–81
24. Madelin G, Lee JS, Inati S, Jerschow A, Regatte RR (2010) Sodium inversion recovery MRI of the knee joint in vivo at 7T. *J Magn Reson* 207:42–52
25. Kupce E, Freeman R (1995) Adiabatic pulses for wide-band inversion and broadband pulse. *J Magn Reson A* 115:273–276
26. Magland J, Wehrli FW (2006) Pulse sequence programming in a dynamic visual environment. Proceedings of the Fourteenth Meeting of the International Society for Magnetic Resonance in Medicine in Seattle, WA, USA, 3032
27. Greengard L, Lee JY (2004) Accelerating the nonuniform fast Fourier transform. *SIAM Rev* 46:443–454
28. Madelin G, Kline R, Walvick R, Regatte RR (2014) A method for estimating intracellular sodium concentration and extracellular volume fraction in brain in vivo using sodium magnetic resonance imaging. *Sci Rep* 4:4763
29. Madelin G, Jerschow A, Regatte RR (2012) Sodium relaxation times in the knee joint in vivo at 7T. *NMR Biomed* 25:530–537
30. Borthakur A, Shapiro EM, Akella SV, Gougoutas A, Kneeland JB, Reddy R (2002) Quantifying sodium in the human wrist in vivo by using MR imaging. *Radiology* 224:598–602
31. Wheaton AJ, Borthakur A, Shapiro EM, Regatte RR, Akella SV, Kneeland JB et al (2004) Proteoglycan loss in human knee cartilage: quantitation with sodium MR imaging—feasibility study. *Radiology* 231:900–905
32. Shepherd DE, Seedhom BB (1999) Thickness of human articular cartilage in joints of the lower limb. *Ann Rheum Dis* 58:27–34
33. Pipe JG, Zwart NR, Aboussouan EA, Robison RK, Devaraj A, Johnson KO (2011) A new design and rationale for 3D orthogonally oversampled k-space trajectories. *Magn Reson Med* 66:1303–1311
34. Boada FE, Gillen JS, Shen GX, Chang SY, Thulborn KR (1997) Fast three dimensional sodium imaging. *Magn Reson Med* 37:706–715
35. Lustig M, Donoho D, Pauly JM (2007) Sparse MRI: the application of compressed sensing for rapid MR imaging. *Magn Reson Med* 58:1182–1195
36. Madelin G, Chang G, Otazo R, Jerschow A, Regatte RR (2012) Compressed sensing sodium MRI of cartilage at 7T: preliminary study. *J Magn Reson* 214:360–365
37. Madelin G, Babb JS, Xia D, Chang G, Jerschow A, Regatte RR (2012) Reproducibility and repeatability of quantitative sodium magnetic resonance imaging in vivo in articular cartilage at 3 T and 7 T. *Magn Reson Med* 68:841–849
38. Insko EK, Kaufman JH, Leigh JS, Reddy R (1999) Sodium NMR evaluation of articular cartilage degradation. *Magn Reson Med* 41:30–34
39. Ku HH (1966) Notes on the use of propagation of error formulas. *J Res Natl Bur Stand* 70C:263–273